Facile Preparation of Free-Standing Carbon Nanotube Arrays Produced Using Two-Step Floating-Ferrocene Chemical Vapor Deposition

Xiaoshuang Yang,[†,‡] Lixiang Yuan,[†,*] Vanessa K. Peterson,[‡] Andrew I. Minett,[†] Yongbai Yin,[§] and Andrew T. Harris[†]

[†]Laboratory for Sustainable Technology, School of Chemical and Biomolecular Engineering, Building J01, University of Sydney, NSW 2006, Australia

[‡]The Bragg Institute, Australian Nuclear Science and Technology Organisation, Lucas Heights, NSW 2234, Australia, and

[§]Applied and Plasma Physics Group, School of Physics, University of Sydney, NSW 2006, Australia

ABSTRACT: A two-step floating-ferrocene chemical vapor deposition method has been devised for the preparation of single-layered aligned carbon nanotube (CNT) arrays. In the first step, uniform Fe catalysts are in situ produced and coated on a Si substrate from ferrocene; single-layered CNT arrays are prepared on these catalysts from ethylene in the second step. The effect of ferrocene loading on the distribution of Fe catalysts, as well as the morphology, diameter, and height of the CNT arrays, was investigated. A novel vacuum extraction process was employed to release the as-prepared CNT array from the Si wafer after water etching at 750 °C. The structural integrity of the free-standing arrays was preserved after the detachment process. The interface between the substrate and the as-grown CNT array was examined. The Fe catalyst distribution on the Si substrate remained homogeneous when the CNT array was removed, and the tops and bottoms of the arrays had different structures, suggesting that the arrays were formed predominantly by a base-growth mode. These free-standing arrays could potentially be applied in membrane or electronic applications.

KEYWORDS: *ferrocene, floating, aligned carbon nanotube, chemical vapor deposition, single-layered*

1. INTRODUCTION

Carbon nanotubes (CNTs) have been synthesized in various shapes[1] and used in a wide range of applications.[2] Because of their ordered structure and controllable growth, aligned CNT arrays have potential as nanoelectric devices,[3] sensors,[4] and separation membranes for gas and water purification.[5−7] Free-standing aligned CNT arrays without a substrate are important for application in membrane and electronic devices,[8,9] but remain difficult to achieve, because aligned CNT arrays must be released from their growth substrates and transferred to other substrates not compatible with CNT growth. For example, anodic aluminum oxide (AAO) can be used as a template for the growth of aligned CNTs, however, the enhanced gas transport properties of aligned CNTs[6] were not observed in the composite membrane.[10] To use the outstanding properties of aligned CNTs produced on an AAO film for membrane applications, the AAO must be removed. Currently, several methods produce free-standing aligned CNT arrays.[8,11,12] Weak oxidants (H_2O, CO_2) were usually used to open the CNT ends and break the covalent bonding between the CNTs and catalyst.[11,13]

Many synthesis techniques, including thermal chemical vapor deposition (CVD),[14] plasma-enhanced CVD,[15] aerosol-assisted CVD,[16] and floating-catalyst CVD,[17,18] have been developed for the preparation of aligned CNT arrays. Using thermal CVD a high-quality single-layered aligned CNT array can be grown on a flat substrate bearing predeposited metal catalyst. Sputtering and electron beam evaporation are normally employed to predeposit the metal layer for catalyst formation. Though thermal CVD is very controllable, it is complex and expensive. Rather than using catalyst predeposition, floating-catalyst CVD continuously grows CNTs from the gas phase onto a substrate by simultaneously introducing the catalyst precursor and carbon source. Thus, floating CVD synthesis has attracted attention for the production of CNT arrays due to its low cost and facile fabrication process, as well as its scalability. However, there are several disadvantages of using floating CVD to produce CNT arrays, such as the production of multilayered CNT arrays,[19] in which the discontinuous structure may block gas or water transport through the inner channels of the vertical CNTs or affect the electron transport along the CNTs.

The properties of aligned CNT arrays vary with the CNT diameter and height. In particular, some researchers have concluded that the conductivity and field emission characteristics of an array depend strongly on the CNT diameter.[20,21] Precise control over CNT array height is also essential for biomedical and other applications.[22−24] The catalyst size and distribution on the substrate determine the diameter and wall number of the CNTs that grow,[25] and strategies developed to control the catalyst include controlling the catalyst layer thickness[25] and chemical treatment of the catalyst.[26] In a floating system, CNT diameter can be modulated by the catalyst-precursor feeding rate. Singh et al.[27] and Bai et al.[28] found that the diameters of CNTs formed by a floating method
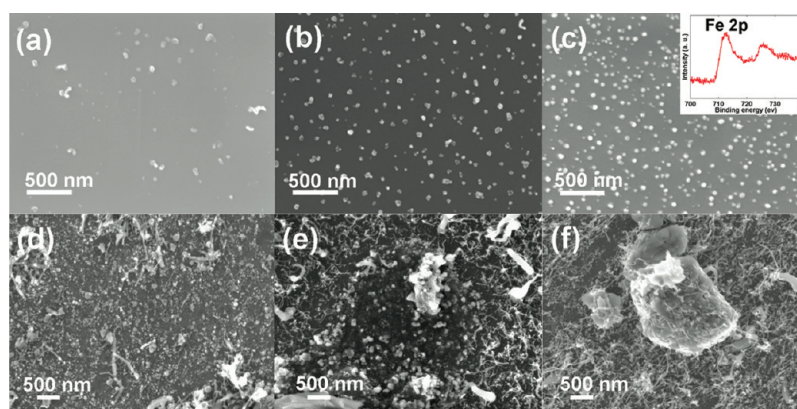
Figure 1. SEM images of the substrate surface after ferrocene dissociation at the loading of (a) 25, (b) 50, (c) 100, (d) 150, (e) 200, and (f) 300 mg; inset in (c) shows the XPS spectrum of the B100 surface.

were proportional to the ferrocene concentration in the feed solution. Zhang et al. adjusted the ferrocene feeding rate by changing the evaporation temperature and thus controlled the diameter of as-grown CNTs.[29]

The injection method is usually used to introduce precursors into a conventional floating-catalyst CVD system for the synthesis of CNT arrays. However, when the injection method is used with floating-catalyst CVD, both catalyst and carbon feedstocks are introduced simultaneously, yielding poor control over the morphology and alignment of the resultant CNT array. For example, CNT arrays synthesized by the injection method lack uniformity and form multilayers,[19,30] neither of which are favorable for some applications. To overcome such problems in the production of CNT arrays using conventional floating-catalyst CVD, we have developed a two-step floating CVD protocol using ferrocene as the catalyst precursor and separating the catalyst preparation and CNT synthesis into sequential steps. This two-step method enables control of the catalyst distribution, and consequently, allows single-layered CNT arrays to be produced. The single-layered CNT arrays prepared by two-step floating-ferrocene CVD were easily detached from the substrates by water etching followed by a novel vacuum extraction process, yielding free-standing aligned CNT arrays. This combination of improved control during the synthesis of aligned CNT arrays with a method for simple, controllable detachment, is a step toward the scalable development of aligned CNT technologies.

2. EXPERIMENTAL SECTION

2.1. Synthesis of Single-Layered CNT Arrays. A dual-zone furnace (OTF-1200 × 2-II, MTI) fitted with a quartz tube (ID = 44 mm, length = 1000 mm) was employed for CNT array growth. Ferrocene (98%, Sigma Aldrich) was placed in a ceramic boat in the first zone, and the synthesis of both Fe catalyst and CNT arrays was carried out in the second zone. A small Si wafer (5 mm ×5 mm) with a 10-nm thick Al_2O_3 coating was used as the substrate for CNT array growth. The flow rates of Ar (99.99%, Coregas), H_2 (99.99%, Coregas) and C_2H_4 (99.8%, Coregas) were controlled via separate mass flow controllers (Alicat Scientific 16 Series). At ambient temperature and atmospheric pressure, the system was first purged with 1000 sccm Ar for 20 min. The flow of Ar was lowered to 500 sccm, and the first zone was heated to 250 °C over 75 min to evaporate ferrocene while the second zone was ramped to 750 °C during the same period. The zones were then maintained at the same temperatures while a 400/140/115 sccm $H_2/Ar/C_2H_4$ mixture was introduced, feeding CNT growth. After 30 min growth, the furnace was cooled to ambient temperature under a flow of 500 sccm Ar.

Different ferrocene loadings (25, 50, 100, 150, 200, and 300 mg) were used. A set of blank samples was prepared to allow for analysis of the catalyst at each ferrocene loading by quickly cooling the furnace within 15 min after it reached 750 °C without adding C_2H_4 or H_2. The quartz tube was cleaned after each run; a run consisted of catalyst synthesis and CNT array growth.

2.2. Preparation of Single-Layered, Free-Standing CNT Arrays. A CNT array was prepared by the two-step floating CVD method using 100 mg ferrocene as the catalyst precursor and one hour of growth at 750 °C. The as-synthesized, single-layered CNT array was water-etched in the same tube furnace used for its synthesis. The furnace was ramped to 750 °C over 75 min under 500 sccm Ar, then 400 sccm Ar was introduced through a water bubbler for 20 min. The furnace was then cooled to room temperature in 500 sccm Ar.

After water etching, the CNT/substrate composite was fixed onto a flat surface using double-sided adhesive. A tube capped with a filtration membrane was placed ~1 mm above the CNT array, and a vacuum was applied in the tube using a pump. The CNT array was abruptly drawn from the substrate onto the filtration membrane. After the vacuum was stopped, the free-standing CNT array could easily be removed from the filtration membrane.

2.3. Characterization Methods. The morphology of the aligned CNT arrays as well as the morphology and distribution of the Fe catalyst on the blank samples was measured using field emission scanning electron microscopy (SEM, Zeiss Ultra plus). The diameter distribution of the CNTs was analyzed statistically from measurements of 50 tubes using high resolution transmission electron microscopy (HRTEM, Philips CM120 Biofilter). Chemical analysis of the surface of the substrate after detatchment of the CNT array was carried out using X-ray photoelectron spectroscopy (XPS) with an ESCALA-B220i-XL probe.

3. RESULTS AND DISCUSSION

3.1. Catalyst Particle Characterization. The two-step floating-ferrocene CVD technique presented here is somewhat similar to thermal CVD, in which the CNT growth process begins with the formation of catalyst particles from the predeposited metal film.[31] Unlike using thermal CVD, using the two-step floating ferrocene CVD method to produce CNT arrays produces particulate catalyst that is coated in situ. Fe catalyst particles were produced using two-step floating ferrocene CVD by the dissociation of ferrocene at temperatures higher than 500 °C[32] before the temperature was ramped to 750 °C for CNT synthesis. In order to understand the effect of ferrocene loading on the catalyst morphology and distribution, a set of catalyst samples was prepared by heating the furnace to 750 °C, then rapidly cooling to ambient temperature in Ar without introducing a carbon feedstock. The samples produced

1418

dx.doi.org/10.1021/am201673v | ACS Appl. Mater. Interfaces 2012, 4, 1417−1422
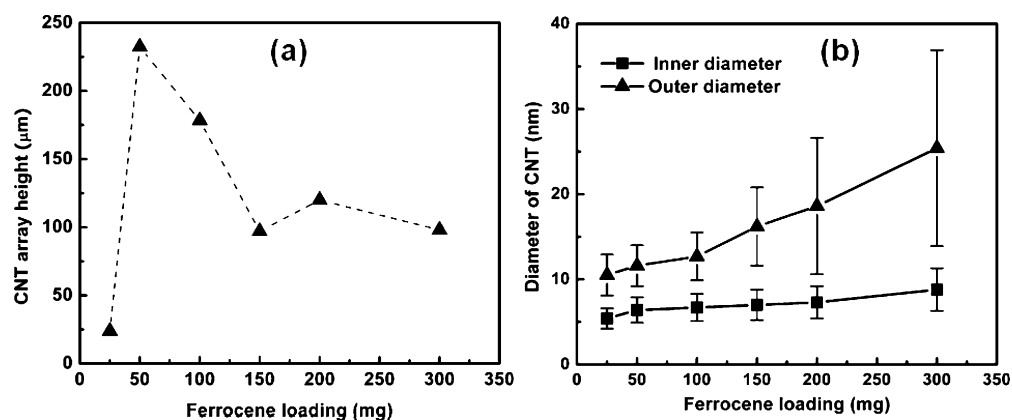
Figure 2. (a) CNT array height as a function of ferrocene loading; (b) inner and outer diameters of CNTs in arrays as a function of ferrocene loading.

from ferrocene loadings of 25, 50, 100, 150, 200, and 300 mg are denoted B25, B50, B100, B150, B200, and B300, respectively, and were characterized by SEM (Figure 1). In sample B25, only a few catalyst particles were found scattered on the Si surface (Figure 1a) and the particle size was calculated as 30.3 nm using SEM analysis. As the amount of ferrocene was increased to 50 and then 100 mg (Figure 1b and c, respectively), more catalyst particles were produced and these were spaced more closely. The particle size in B50 and B100 increased to 33.1 and 36.3 nm, respectively. Additionally, they were homogeneously distributed (Figure 1a−c). The X-ray photoelectron spectroscopy (XPS) of B100 (Figure 1c, inset) clearly proved that the particles on Si surface were Fe. The nanosized metallic Fe catalyst particles are oxidized upon their removal from the furnace and the Fe2p XPS signal appearing at ~712 eV evidences the presence of iron oxide.[33] Using more ferrocene enhances the catalyst particle density on the substrate (Figure 1d−f), and at the highest loadings, the distribution of particles on the substrate became irregular. At some sites, Fe particles were coated repeatedly because of the continuous decomposition of ferrocene, leading to catalyst aggregates. At other sites, only a few Fe particles were coated, forming smaller aggregates. Because of the Ostwald ripening effect,[34] small particles tend to coarsen into large particles; this effect was obvious in samples B150−B300. As a result, the size distribution of catalyst particles was broader when more ferrocene was used. For example, in sample B300, particles with a diameter range of 40 nm to several micrometers were found. It is important to note that short CNTs or carbon fibres were observed on the catalyst particles in some regions of samples B150−B300 (Figure 1d−f); these most likely grew from carbon compounds released during the ferrocene decomposition.

In this study, metallic Fe particles were obtained when ferrocene was treated at temperatures higher than 500 °C, and even at 400 °C,[35] despite the fact that thermodynamic calculations suggest that the decomposition cannot occur below 800 °C in the absence of H_2 or a catalyst.[36] However, a recent study suggest that the dissociation of ferrocene is a complex process involving several possible routes.[37] Furthermore, ferrocene decomposes into hydrocarbons and Fe clusters, which may further catalyze ferrocene decomposition.[35] This autocatalysis allows the Fe catalyst to be formed and coated in situ in a separate step prior to CNT growth.

3.2. Properties of the As-Synthesized CNT Arrays.

CNT arrays grown on catalysts produced from 25, 50, 100, 150, 200, and 300 mg ferrocene are denoted S25, S50, S100, S150, S200, S250, and S300, respectively. The relationship between CNT array height and ferrocene loading is shown in Figure 2a. At a very low ferrocene loading (S25), the CNTs were short and sparse and did not fully cover the substrate. When the ferrocene loading increased to 50 mg, the CNT array (S50) height increased significantly, from 24 to 232 μm. Further increases in ferrocene loading up to 150 mg decreased the array height (S100 and S150), and the heights of CNT arrays S150, S200, and S300 were relatively similar at approximately 110 μm. Malek Abbaslou et al. showed that in a floating-ferrocene CVD system the CNT yield was increased when the ferrocene concentration increased.[38] However, the CNT growth was inhibited when ferrocene loading exceeded 100 mg due to catalyst deactivation caused by particle agglomeration and carbon deposition from ferrocene (Figure 1d−f). Controlled CNT growth was reported using a one-step floating-ferrocene CVD method, where the density of Fe catalysts affected the length and tube diameter of CNTs in vertical arrays.[39] This work supports our findings that S50 was the highest array, reaching 232 μm with an average growth rate of 7.7 μm/min.

TEM measurements were conducted to study the relationship between ferrocene loading and CNT diameter. Figure 2b shows the CNT diameter distribution from 50 CNTs in each TEM sample. As the ferrocene loading increased from 25 to 300 mg, the average outer diameter of CNTs increased considerably from 10.5 to 25.4 nm, whereas the inner diameter increased from 5.4 to 8.8 nm. Furthermore, the standard deviation of the average diameter increased with a similar trend, so the size distribution was broader when more ferrocene was added. In the conventional production of CNTs using floating-ferrocene CVD, the CNT diameter is controlled by adjusting the catalyst precursor concentration[28,39] or the sublimation temperature,[29] both of which enlarge the diameter of as-synthesized CNTs by increasing the ferrocene feeding rate. However, the CNT diameters cannot be correlated to the catalyst particle size using this conventional floating CVD method because the size distribution of the catalyst particles are difficult to measure.[28,29] The CNTs produced using 25, 50, and 100 mg of ferrocene have diameters (10.5, 11.6, and 12.7 nm, respectively) that increase with increasing particle size (30.3, 33.1, and 36.3 nm, respectively), with a constant ratio of 1:2.9. This ratio of CNT diameter to catalyst size is similar to that
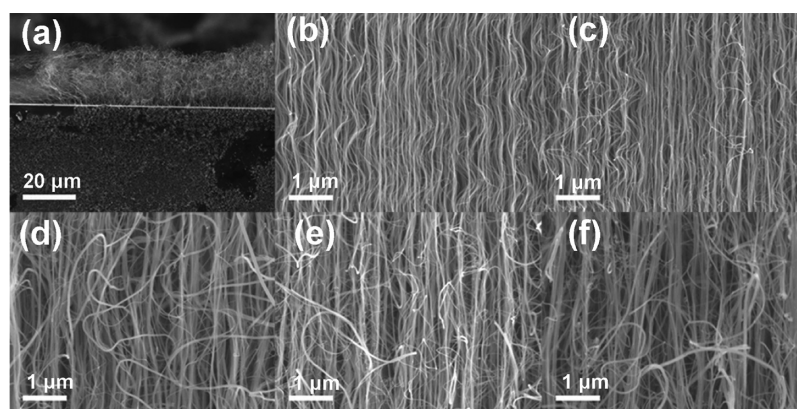
Figure 3. Side-view SEM images of CNT arrays synthesized using different ferrocene loadings: (a) 25, (b) 50, (c) 100, (d) 150, (e) 200, and (f) 300 mg.

previously reported for predeposited catalyst using thermal CVD.[40,41] We note that the catalyst particles in the present study were examined ex situ and the difference in the measured catalyst particle size and the CNT diameter is possibly caused by coarsening of the catalyst particles during cooling. When more ferrocene was used, the broad particle size distribution and presence of deposited carbon precluded quantitative measurements. It is still obvious that more and larger particles were formed when 150, 200, and 300 mg of ferrocene were used (Figure 1).

SEM analysis of the side-views of the as-prepared CNT arrays was conducted to evaluate their alignment (Figure 3). S25 (Figure 3a) shows a short, tangled structure. A crowding effect is necessary to align CNTs in an array[42] as the van der Waals interactions among CNTs maintain their vertical growth orientation.[14] The catalyst density strongly influences the height and morphology of the resulted CNT arrays.[26,39,43] The scarcely distributed catalyst particles in B25 (Figure 1a) resulted in a weak crowding effect. As a result, the growth of CNT array (S25) was inhibited and the alignment was almost lost. As shown in panels b and c in Figure 3, the CNT arrays S50 and S100 exhibited better aligned structures than the others. S50 and S100 were prepared with a higher ferrocene loading than S25, and therefore S50 and S100 had a higher catalyst/carbon ratio and significantly enhanced carbon yield (presented here as CNT array height), relative to S25. The better alignment of S50 and S100 compared to S25 can be attributed to the enhanced crowding effect due to the greater catalyst particle density (Figure 1). More than 100 mg ferrocene caused further catalyst deposition, and SEM analysis shows worsening CNT alignment with ferrocene loading beyond 100 mg. The same trend has been found in other studies and it has been suggested that the CNT growth rate decreases with increasing catalyst particle size, which is in turn controlled by the thickness of the metal film.[25,44] Wei et al. found a critical film thickness (∼40 nm at 760 °C) above which no CNTs would grow on a substrate.[45] McKee et al. proposed when floating-ferrocene CVD is used to produce CNTs a high catalyst concentration causes catalyst particles to grow beyond the threshold for CNT formation.[46] Ionescu et al. reported that an optimal catalyst density for CNT nucleation and growth was obtained at a particular ferrocene concentration using a one-step floating-ferrocene CVD.[39]

**3.3. Preparation of Free-Standing Arrays.** In electronic and membrane applications, free-standing CNT arrays are preferred for assembly. We chose to remove the CNT array from its substrate by water etching, which can break CNT−catalyst bonds[47] and is easier than acidic erosion methods.[5,11] However, after water etching, the CNT array was still difficult to separate from its support while maintaining the array's integrity, perhaps as a result of the remaining van der Waals interaction between the CNT array and the substrate.[48,49] Adhesive tape can be used to release an aligned CNT array from its substrate, however, this results in only partial extraction of the CNTs from the substrate and also creates the requirement to detach the CNT array from the tape.[50] The vacuum extraction method employed here allowed full extraction of the CNT array from its substrate. The schematic of the extraction process is illustrated in Figure 4. As a uniform
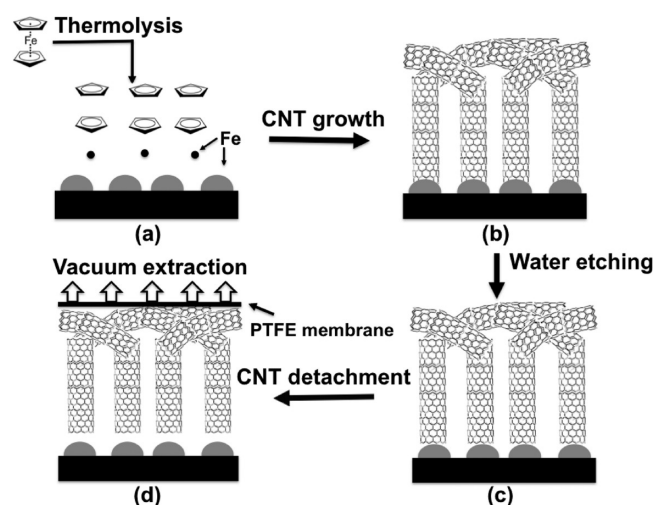
Figure 4. Schematic of the synthesis and detachment of an aligned CNT array: (a) Dissociation of ferrocene and deposition of Fe, (b) growth of the CNT array, (c) water etching of the CNT array, and (d) CNT detachment by vacuum extraction.

vacuum was applied, the structural integrity of the aligned free-standing CNT array was preserved after detachment.

The interface between the CNT array and the substrate was examined. The surface of the substrate after detachment, along with the top and bottom of the free-standing CNT array, are shown in Figure 5. Particles remain homogeneously distributed on the substrate (Figure 5a) and XPS analysis confirmed that these particles were Fe (inset in Figure 5a). This suggests that a
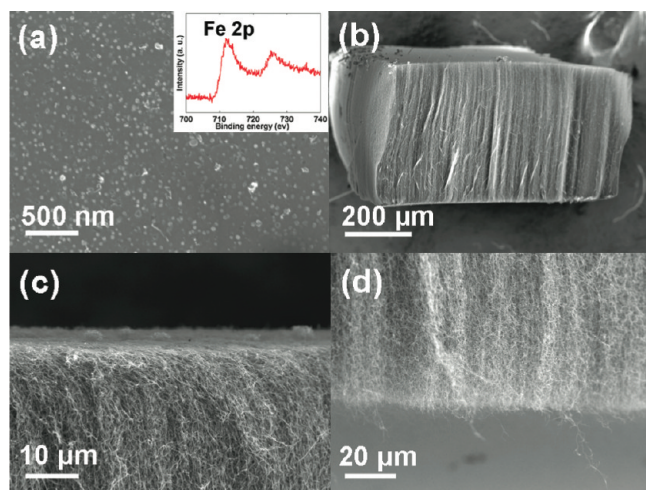
Figure 5. SEM images of (a) the substrate surface after CNT array removal, (b) free-standing CNT array, (c) top and (d) bottom morphologies of a free-standing CNT array. The inset in (a) shows the XPS spectrum of the substrate surface after removal of the CNT array.

base-growth mode was dominant in our two-step floating-ferrocene CVD method and that the detachment technique damaged neither the substrate nor the CNTs. Combined with the SEM and XPS results (Figure 5), TEM images confirm that the as-prepared free-standing CNT array was catalyst-free (Figure 6a) and open-ended (Figure 6b), as demonstrated in
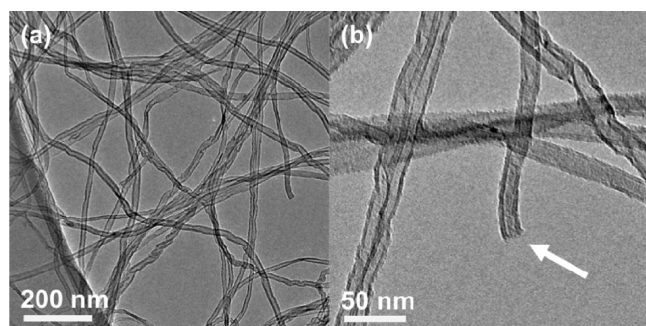
Figure 6. Typical TEM images of (a) the as-prepared free-standing CNTs and (b) an open-ended CNT.

the schematic (Figure 4). The uniform distribution of Fe catalyst on the substrate is similar to that prior to CNT growth (Figure 1c), which suggests that the catalyst particles produced from the ferrocene were bonded to the substrate for the duration of the CNT growth. Few CNTs were formed on the catalyst particles during the first synthesis step at ferrocene loadings below 150 mg (Figure 1a−d). Visual inspection of the ceramic boat confirmed that all ferrocene is consumed in step one and that C_2H_4 is the carbon source that feeds the CNT growth in step two. Hence, the CNT arrays produced from the two-step process with ferrocene loadings below 150 mg were single-layered, similar to the arrays produced by thermal CVD. Aligned CNT arrays produced using conventional floating-catalyst CVD are multilayered.[19] Although multilayered millimeter-high CNT arrays have been prepared for some special applications,[51] single-layered CNT arrays are preferred for membrane and other applications that need continuous and uniform CNTs along the vertical direction. The two-step floating ferrocene CVD method employed here is economic

and controllable and produces single-layered CNT arrays. The free-standing CNT array is shown in Figure 5b and its height was estimated to be 420 μm, almost twice as high as S100 as a result of a growth time double that of S100. Interestingly, the free-standing CNT array exhibited different morphologies at its top and bottom. At the top, the CNTs gathered together and were tangled into a crust; no individual CNT was distinguishable (Figure 5c). Given that the array grew via base growth, the crust was formed at the initial stage of CNT growth and pushed up during the growth process, in accordance with previous studies.[52] On the bottom of the free-standing array, the CNTs were well-separated and seldom intertwined (Figure 5d). These CNTs were originally anchored on Fe particles and apparently remained separate after the water etching and final detachment process.

4. CONCLUSIONS

Single-layered, aligned CNT arrays with tailored morphologies and diameters were synthesized by a two-step floating-ferrocene CVD method. The morphology and distribution of Fe catalyst particles could be controlled by changing the ferrocene loading in the first step of the method. As a result, the height, diameter, and alignment of the as-synthesized CNT arrays obtained in the second step were modulated by the changes to the catalyst made in the first step. Single-layered CNT arrays were synthesized when ferrocene loading was below 150 mg. A free-standing CNT array was obtained by detaching the as-synthesized CNT array from the substrate using water etching and vacuum extraction. The as-prepared single-layered, free-standing array should be suitable for membrane assembly for application in gas or water separation.

■ AUTHOR INFORMATION

Corresponding Author
*E-mail: lixiang.yuan@sydney.edu.au.
Notes
The authors declare no competing financial interest.

■ ACKNOWLEDGMENTS

■ REFERENCES

(1) Zhang, M.; Li, J. *Mater. Today* **2009**, *12*, 12.
(2) Baughman, R. H.; Zakhidov, A. A.; De Heer, W. A. *Science* **2002**, *297*, 787.
(3) Hong, S.; Myung, S. *Nat. Nanotechnol.* **2007**, *2*, 207.
(4) Ding, D.; Chen, Z.; Rajaputra, S.; Singh, V. *Sens Actuators, B* **2007**, *124*, 12.
(5) Hinds, B. J.; Chopra, N.; Rantell, T.; Andrews, R.; Gavalas, V.; Bachas, L. G. *Science* **2004**, *303*, 62.
(6) Holt, J. K.; Park, H. G.; Wang, Y.; Stadermann, M.; Artyukhin, A. B.; Grigoropoulos, C. P.; Noy, A.; Bakajin, O. *Science* **2006**, *312*, 1034.
(7) Kim, S.; Jinschek, J. R.; Chen, H.; Sholl, D. S.; Marand, E. *Nano Lett.* **2007**, *7*, 2806.
(8) Murakami, Y.; Maruyama, S. *Chem. Phys. Lett.* **2006**, *422*, 575.
(9) Yu, M.; Funke, H. H.; Falconer, J. L.; Noble, R. D. *Nano Lett.* **2009**, *9*, 225.
(10) Altalhi, T.; Ginic-Markovic, M.; Han, N.; Clarke, S.; Losic, D. *Membranes* **2010**, *1*, 37.

(11) Pint, C. L.; Xu, Y. Q.; Pasquali, M.; Hauge, R. H. *ACS Nano* **2008**, *2*, 1871.

(12) Zhang, G.; Mann, D.; Zhang, L.; Javey, A.; Li, Y.; Yenilmez, E.; Wang, Q.; McVittie, J. P.; Nishi, Y.; Gibbons, J.; Dai, H. *Proc. Natl. Acad. Sci. U.S.A.* **2005**, *102*, 16141.

(13) Yang, X.; Yuan, L.; Peterson, V. K.; Yin, Y.; Minett, A. I.; Harris, A. T. *J. Phys. Chem. C* **2011**, *115*, 14093.

(14) Fan, S.; Chapline, M. G.; Franklin, N. R.; Tombler, T. W.; Cassell, A. M.; Dai, H. *Science* **1999**, *283*, 512.

(15) Chhowalla, M.; Teo, K. B. K.; Ducati, C.; Rupesinghe, N. L.; Amaratunga, G. A. J.; Ferrari, A. C.; Roy, D.; Robertson, J.; Milne, W. I. *J. Appl. Phys.* **2001**, *90*, 5308.

(16) Zhang, Y.; Li, R.; Liu, H.; Sun, X.; Merel, P.; Desilets, S. *Appl. Surf. Sci.* **2009**, *255*, 5003.

(17) Andrews, R.; Jacques, D.; Rao, A. M.; Derbyshire, F.; Qian, D.; Fan, X.; Dickey, E. C.; Chen, J. *Chem. Phys. Lett.* **1999**, *303*, 467.

(18) Hou, H.; Schaper, A. K.; Jun, Z.; Weller, F.; Greiner, A. *Chem. Mater.* **2003**, *15*, 580.

(19) Yang, Z.; Chen, X.; Nie, H.; Zhang, K.; Li, W.; Yi, B.; Xu, L. *Nanotechnology* **2008**, 19.

(20) Li, H. J.; Lu, W. G.; Li, J. J.; Bai, X. D.; Gu, C. Z. *Phys. Rev. Lett.* **2005**, *95*, 086601.

(21) Chhowalla, M.; Ducati, C.; Rupesinghe, N. L.; Teo, K. B. K.; Amaratunga, G. A. *J. Appl. Phys. Lett.* **2001**, *79*, 2079.

(22) Correa-Duarte, M. A.; Wagner, N.; Rojas-Chapana, J.; Morsczeck, C.; Thie, M.; Giersig, M. *Nano Lett.* **2004**, *4*, 2233.

(23) Constantopoulos, K. T.; Shearer, C. J.; Ellis, A. V.; Voelcker, N. H.; Shapter, J. G. *Adv. Mater.* **2010**, *22*, 557.

(24) Andrews, R.; Jacques, D.; Qian, D.; Rantell, T. *Acc. Chem. Res.* **2002**, *35*, 1008.

(25) Zhao, B.; Futaba, D. N.; Yasuda, S.; Akoshima, M.; Yamada, T.; Hata, K. *ACS Nano* **2009**, *3*, 108.

(26) Nessim, G. D.; Hart, A. J.; Kim, J. S.; Acquaviva, D.; Oh, J.; Morgan, C. D.; Seita, M.; Leib, J. S.; Thompson, C. V. *Nano Lett.* **2008**, *8*, 3587.

(27) Singh, C.; Shaffer, M. S. P.; Windle, A. H. *Carbon* **2003**, *41*, 359.

(28) Bai, S.; Li, F.; Yang, Q. H.; Cheng, H. M.; Bai, J. B. *Chem. Phys. Lett.* **2003**, *376*, 83.

(29) Zhang, Q.; Huang, J. Q.; Zhao, M. Q.; Qian, W. Z.; Wei, F. *Appl. Phys. A: Mater. Sci. Process.* **2009**, *94*, 853.

(30) Kunadian, I.; Andrews, R.; Qian, D.; Pinar Mengüç, M. *Carbon* **2009**, *47*, 384.

(31) Meshot, E. R.; Plata, D. L.; Tawfick, S.; Zhang, Y.; Verploegen, E. A.; Hart, A. J. *ACS Nano* **2009**, *3*, 2477.

(32) Barreiro, A.; Hampel, S.; Rummeli, M. H.; Kramberger, C.; Gruneis, A.; Biedermann, K.; Leonhardt, A.; Gemming, T.; Buchner, B.; Bachtold, A.; Pichler, T. *J. Phys. Chem. B* **2006**, *110*, 20973.

(33) Beck, U.; Hertwig, A.; Kormunda, M.; Krause, A.; Krüger, H.; Lohse, V.; Nooke, A.; Pavlik, J.; Steinbach, J. r. *Sens. Actuators, B* **2011**, *160*, 609.

(34) Amama, P. B.; Pint, C. L.; McJilton, L.; Kim, S. M.; Stach, E. A.; Murray, P. T.; Hauge, R. H.; Maruyama, B. *Nano Lett.* **2009**, *9*, 44.

(35) Dyagileva, L. M.; Mar'in, V. P.; Tsyganova, E. I.; Razuvaev, G. A. *J. Organomet. Chem.* **1979**, *175*, 63.

(36) Kuwana, K.; Saito, K. *Proc. Combust. Inst.* **2007**, *31*, 1857.

(37) Leonhardt, A.; Hampel, S.; Muller, C.; Monch, I.; Koseva, R.; Ritschel, M.; Elefant, D.; Biedermann, K.; Buchner, B. *Chem. Vap. Deposition* **2006**, *12*, 380.

(38) Malek Abbaslou, R. M.; Soltan, J.; Dalai, A. K. *Appl. Catal., A* **2010**, *372*, 147.

(39) Ionescu, M. I.; Zhang, Y.; Li, R.; Sun, X.; Abou-Rachid, H.; Lussier, L. S. *Appl. Surf. Sci.* **2011**, *257*, 6843.

(40) Cui, X.; Wei, W.; Harrower, C.; Chen, W. *Carbon* **2009**, *47*, 3441.

(41) Nikolaev, P.; Bronikowski, M. J.; Bradley, R. K.; Rohmund, F.; Colbert, D. T.; Smith, K. A.; Smalley, R. E. *Chem. Phys. Lett.* **1999**, *313*, 91.

(42) Patole, S. P.; Alegaonkar, P. S.; Shin, H. C.; Yoo, J. B. *J. Phys. D: Appl. Phys.* **2008**, 41.

(43) Bennett, R. D.; Hart, A. J.; Cohen, R. E. *Adv. Mater.* **2006**, *18*, 2274.

(44) Wang, Y.; Luo, Z.; Li, B.; Ho, P. S.; Yao, Z.; Shi, L.; Bryan, E. N.; Nemanich, R. J. *J. Appl. Phys.* **2007**, 101.

(45) Wei, Y. Y.; Eres, G.; Merkulov, V. I.; Lowndes, D. H. *Appl. Phys. Lett.* **2001**, *78*, 1394.

(46) McKee, G. S. B.; Deck, C. P.; Vecchio, K. S. *Carbon* **2009**, *47*, 2085.

(47) Hata, K.; Futaba, D. N.; Mizuno, K.; Namai, T.; Yumura, M.; Iijima, S. *Science* **2004**, *306*, 1362.

(48) Qu, L.; Dai, L.; Stone, M.; Xia, Z.; Zhong, L. W. *Science* **2008**, *322*, 238.

(49) Autumn, K.; Sitti, M.; Liang, Y. A.; Peattie, A. M.; Hansen, W. R.; Sponberg, S.; Kenny, T. W.; Fearing, R.; Israelachvili, J. N.; Full, R. J. *Proc. Natl. Acad. Sci. U.S.A.* **2002**, *99*, 12252.

(50) Qu, L.; Zhao, Y.; Hu, Y.; Zhang, H.; Li, Y.; Guo, W.; Luo, H.; Dai, L. *J. Mater. Chem.* **2010**, *20*, 3595.

(51) Zhu, L.; Xiu, Y.; Hess, D. W.; Wong, C. P. *Nano Lett.* **2005**, *5*, 2641.

(52) De Volder, M. F. L.; Vidaud, D. O.; Meshot, E. R.; Tawfick, S.; John Hart, A. *Microelectron. Eng.* **2010**, *87*, 1233.